

## Phase-Transformation Wave Dynamics in LiFePO<sub>4</sub>

Damian Burch<sup>1,a</sup>, Gogi Singh<sup>1,b</sup>, Gerbrand Ceder<sup>2,c</sup> and Martin Z. Bazant<sup>1,d</sup>

<sup>1</sup>Department of Mathematics

<sup>2</sup>Department of Materials Science and Engineering

Massachusetts Institute of Technology, Cambridge, MA 02139, USA

<sup>a</sup>burch@math.mit.edu, <sup>b</sup>gogi@math.mit.edu, <sup>c</sup>gceder@mit.edu, <sup>d</sup>bazant@math.mit.edu

**Keywords:** LiFePO<sub>4</sub>, continuum modeling, phase transformations, wave dynamics, defects

**Abstract.** A general continuum model has recently been proposed for the dynamics of ion intercalation in a single crystal of rechargeable-battery electrode materials [1]. When applied to strongly phase-separating, highly anisotropic materials such as LiFePO<sub>4</sub>, phase-transformation waves are predicted between the lithiated and unlithiated portions of a crystal. In this paper, we extend the analysis of the wave dynamics, and we describe a new mechanism for current capacity fade through the interactions of these waves with defects in the material.

### Introduction

LiFePO<sub>4</sub> is a promising cathode material for safe, high-power Li-ion rechargeable batteries [2]. Until recently, the only theory available to describe intercalation dynamics in this material was the isotropic “shrinking core” model [3]. However, first-principles simulations [4] and experiments [5] for LiFePO<sub>4</sub> point to qualitatively different behavior. The shrinking-core model assumes a spherical, bulk phase boundary shrinking in the direction of lithium flux, but in FePO<sub>4</sub> lithium diffusion is limited to one-dimensional channels, which are successively filled or emptied as the LiFePO<sub>4</sub>/FePO<sub>4</sub> interface moves in a direction perpendicular to the flux and spanning the crystal.

A more general continuum model has recently been developed [1]. It is based on basic thermodynamic and kinetic properties of intercalation materials, such as energy costs for partial lithiation, anisotropic nonlinear bulk diffusion, and composition-dependent surface reactions. In certain parameter ranges applicable to LiFePO<sub>4</sub>, the governing equation has wave-like solutions for the phase interface, which are consistent with experimental observations.

In this paper, we will expand on the wave dynamics predicted by this model for phase transformations in the appropriate regime for LiFePO<sub>4</sub>. In particular, whereas Ref. [1] focused on developing the general model and describing flat wave-fronts propagating in an ideal crystal, we will study several phenomena which occur in more realistic, three-dimensional crystals. We will also show that this model reveals a new mechanism for power loss in battery materials resulting from interactions between the phase-transformation waves and material defects.

### The Mathematical Model

We begin by briefly summarizing the general model for single-crystal Li-intercalation phase transformation [1]. Denote by  $c$  the dimensionless, normalized Li concentration, where the unlithiated phase is characterized by  $c \approx 0$  and the lithiated phase by  $c \approx 1$ . The free energy  $F$  of a crystal is approximated by the general Cahn-Hilliard form, where  $c$  act as a phase field [6]

$$F = \iiint_V \left[ \bar{f}(c) + \frac{1}{2} (\nabla c)^T \mathbf{K} (\nabla c) \right] dV \quad (1)$$

Here  $\bar{f}(c)$ ---the *homogeneous free energy density*---is the free energy density of a crystal with uniform concentration  $c$ , which takes the regular solution form [6],

$$\bar{f}(c) = ac(1-c) + \rho k_B T [c \log(c) + (1-c) \log(1-c)] \quad (2)$$

where  $a$  is the average energy density of the interaction between Li ions,  $\rho$  the number of intercalation sites per unit volume,  $k_B$  Boltzmann's constant, and  $T$  the temperature. The first term is an enthalpic contribution, which promotes phase separation, and the second term is an entropic contribution, which promotes mixing. The second term in Eq. (1)---the *gradient penalty*---broadens a phase interface and determines its structure. In general,  $\mathbf{K}$  is a symmetric, positive definite tensor, which must reflect the underlying symmetry of the crystal.

The bulk chemical potential of Li the variational derivative of  $F$  with respect to the concentration

$$\mu = a(1-2c) + \rho k_B T \log\left(\frac{c}{1-c}\right) - \nabla \cdot (\mathbf{K} \nabla c) \quad (3)$$

Note that  $\mu$  is actually  $\rho$  times the chemical potential, or the chemical potential per unit volume; since  $\rho$  is assumed to be constant. We continue to call this  $\mu$  the chemical potential. As usual, gradients in the chemical potential act as thermodynamic driving forces for Li diffusion, yielding the Li flux  $\mathbf{j} = -c \mathbf{B} \nabla \mu$  ( $\mathbf{B}$  is the mobility tensor which, in general, is highly anisotropic and concentration-dependent). This must satisfy local conservation, i.e.  $\rho \frac{\partial c}{\partial t} + \nabla \cdot \mathbf{j} = 0$ .

To describe Li transfer with the surrounding electrolyte, Ref. [1] proposes Arrhenius kinetics driven by *chemical potential differences*, which (unlike the standard Butler-Volmer approach) depend on  $c$  and its gradient at the surface via (3). In particular, the rate of Li insertion at the surface of the crystal is given by  $R_{ins} = k_{ins} c_e \exp\left[\frac{(\mu_e - \mu)}{\rho k_B T}\right]$ , where  $k_{ins}$  is the insertion rate coefficient,  $c_e$  is the Li concentration in the electrolyte, and  $\mu_e$  is the Li (ion) chemical potential in the electrolyte. Similarly, the rate of Li extraction is given by  $R_{ext} = k_{ext} c \exp\left[\frac{(\mu - \mu_e)}{\rho k_B T}\right]$ , where  $k_{ext}$  is the extraction rate coefficient. Defining the *net* insertion rate by  $R = R_{ins} - R_{ext}$  then yields the boundary condition  $\hat{\mathbf{n}} \cdot \mathbf{j} = -\rho_s R$  for the conservation equation; here  $\hat{\mathbf{n}}$  is the outward unit normal at the boundary and  $\rho_s$  is the number of intercalation sites per unit area on the surface.

The last step of the analysis in [1] is to specialize to the *surface-reaction-limited* (SRL) regime appropriate for LiFePO<sub>4</sub>. Define the Damkohler number  $Da_x$  to be the ratio of the timescale  $t_x^D$  for diffusion in the x-direction to the timescale  $t^R$  for the surface reaction rates, and similarly define  $Da_y$  and  $Da_z$ . Motivated by *ab initio* calculations [4] predicting that x- and z-diffusion is very slow relative to y-diffusion, as well as by experiments [5] which suggest that the phase-boundary dynamics are limited by reaction rates, we make the assumption that  $Da_x, Da_z \gg 1 \gg Da_y$ . In this regime, Li is confined to 1D channels of fast diffusion. For each such channel, we define the average Li concentration

$$\bar{c}(x, z, t) = \frac{1}{L_y(x, z)} \int c(x, y, z, t) dy \quad (4)$$

where  $L_y$  is the length of the channel. Then depth-averaging the conservation equation and using the above boundary condition leads to the equation governing SRL dynamics

$$\begin{aligned} \frac{\rho L_y}{2\rho_s} \frac{\partial \bar{c}}{\partial t} &= k_{ins} c_e \frac{1-\bar{c}}{\bar{c}} \exp \left[ \frac{\mu_e}{\rho k_B T} - \frac{a}{\rho k_B T} (1-2\bar{c}) + \frac{1}{\rho k_B T} \nabla \cdot (\mathbf{K} \nabla \bar{c}) \right] \\ -k_{ext} \frac{\bar{c}^2}{1-\bar{c}} \exp \left[ -\frac{\mu_e}{\rho k_B T} + \frac{a}{\rho k_B T} (1-2\bar{c}) - \frac{1}{\rho k_B T} \nabla \cdot (\mathbf{K} \nabla \bar{c}) \right] \end{aligned} \quad (5)$$

## Wave Solutions

As argued mathematically in [1], there is a range of physical parameters over which Eq. 5 admits wave solutions. In this section, we briefly expand on the previous discussion.

First, note that the numerical solutions in [1] behave very much as expected on more physical grounds [5]: despite the fact that Li only really moves in the  $y$ -direction, the phase boundary moves in the  $x$ -direction because *net* Li insertion only takes place at the phase interface. This may be understood in terms of the chemical potentials from Eq. 3 (see Fig. 1). In the fully-lithiated part of the crystal behind a lithiation wave, the internal and external chemical potentials are the same (at least when the insertion and extraction rates are equal), so there is no net insertion. In the nearly unlithiated part of the crystal ahead of a lithiation wave, the internal chemical potential for insertion of single Li ions is high due to the lack of lithiated nuclei; however, the concentration is very low, so we again get a steady state. At the phase boundary, the gradient penalty term becomes important and sharply reduces the chemical potential, thus promoting net insertion.

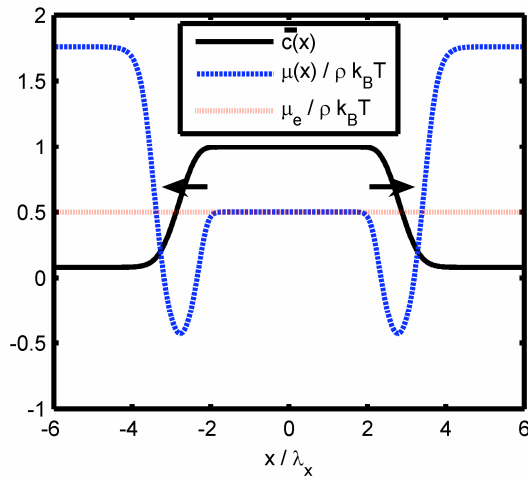


**Figure 1.** This is a 1D numerical simulation of Li insertion waves in the SRL regime (uniformity in the  $z$ -direction is assumed). The solid black line gives the Li concentration in the crystal, the dotted red line gives the external chemical potential (assumed to be uniform), and the dashed blue line gives the Li chemical potential in the crystal. The two insertion waves are spreading outward. In terms of the parameters from [1], we are using  $\tilde{a} = 5, \tilde{\mu}_e = 0.5, \kappa = 1$ .

Second, note that in the one-dimensional simulations studied in [1], the gradient penalty tensor becomes a scalar. In two dimensions, however, this is not the case, and we must consider what impact its anisotropy may have on the wave dynamics. In an orthorhombic crystal, the gradient penalty tensor must be diagonal. We will further assume that it is constant, and write

$$\mathbf{K} = \rho k_B T \begin{pmatrix} \lambda_x^2 & 0 & 0 \\ 0 & \lambda_y^2 & 0 \\ 0 & 0 & \lambda_z^2 \end{pmatrix} \quad (6)$$

where the  $\lambda$ s are length scales characterizing gradient penalties for their respective directions (in the SRL regime,  $\lambda_y$  is ignored).

In  $\text{LiFePO}_4$ , there is relatively weak bonding between  $bc$  layers [5]. We therefore expect that concentration gradients in the  $x$ -direction will not be as heavily penalized as gradients in the  $z$ -direction, i.e. that  $\lambda_z > \lambda_x$ . As shown in [1], the wave velocity in a given direction is directly proportional to the corresponding  $\lambda$ . We therefore expect that lithiation waves will spread much faster in the  $z$ -direction than in the  $x$ -direction. Thus the fact that phase boundaries seen experimentally [5] tend to be aligned along  $bc$ -planes might have a purely dynamical explanation: even if nucleation is localized, lithiation proceeds so quickly in the  $z$ -direction that the wavefront soon spreads across the entire crystal. See Fig. 3 for numerical evidence.

Finally, as mentioned in [1], the wave solutions appear to be very stable numerically. A formal linear stability analysis [7], in fact, reveals that perturbations of wavelength much smaller than  $\lambda_x$  decay exponentially quickly. We will see in the next section that this has important physical consequences.

### Wave-Defect Interactions

One of the most important goals of a mathematical analysis of battery materials is the understanding of battery failure. When studying intercalation dynamics, then, it is natural to ask how the lithiation waves might be disrupted by imperfections in the crystal or in the interface with the electrolyte. In this section, we will focus on localized defects, which we define to mean any physical change in the system, which slows or prevents the filling of a small group of 1-dimensional Li channels. For instance: surface impurities could completely block Li transport into or out of several nearby channels; Fe atoms might occupy some fraction of the Li sites [8], thus reducing the Li capacity of a channel; or imperfect bonding to an electronically conductive phase in the electrolyte might dramatically slow intercalation.

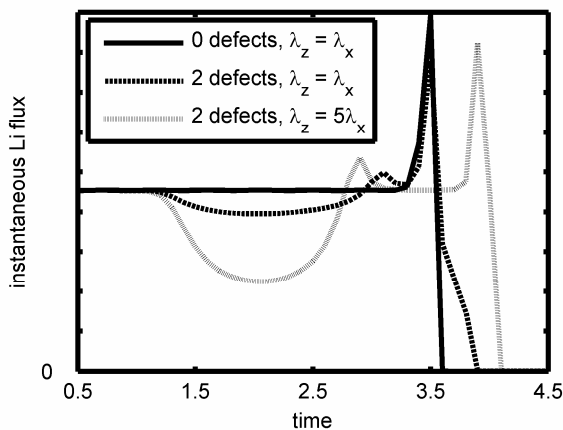


**Figure 2.** The instantaneous Li flux for the three simulations plotted in Fig. 3

From a dynamical point of view, the exact mechanism leading to localized defects is unimportant. When a lithiation wave approaches such a defect, it obviously must bend around it in order to proceed. However, this bending is energetically costly because of the gradient penalty term in Eq. 1: not only does the bend introduce new gradients, but it makes the phase boundary---along which there are already sharp gradients---longer. This will slow the progression of the phase boundary until the defect has been passed, thus reducing the Li flux that the crystal can support.

The problem becomes even more pronounced when  $\mathbf{K}$  is highly anisotropic since such systems would more heavily penalize an increase in the phase boundary. Moreover, in such cases the wave-defect interaction becomes non-local in the sense that a defect of size  $\lambda_x$  affects the wave out to a distance of  $\lambda_z > \lambda_x$  away. For  $\text{LiFePO}_4$ , where we expect  $\lambda_z$  to be large (see above) and  $\lambda_x$  to be on

the atomic scale (see [1]), this means that an atomic-scale defect can impact the phase-transformation dynamics over the entire crystal.

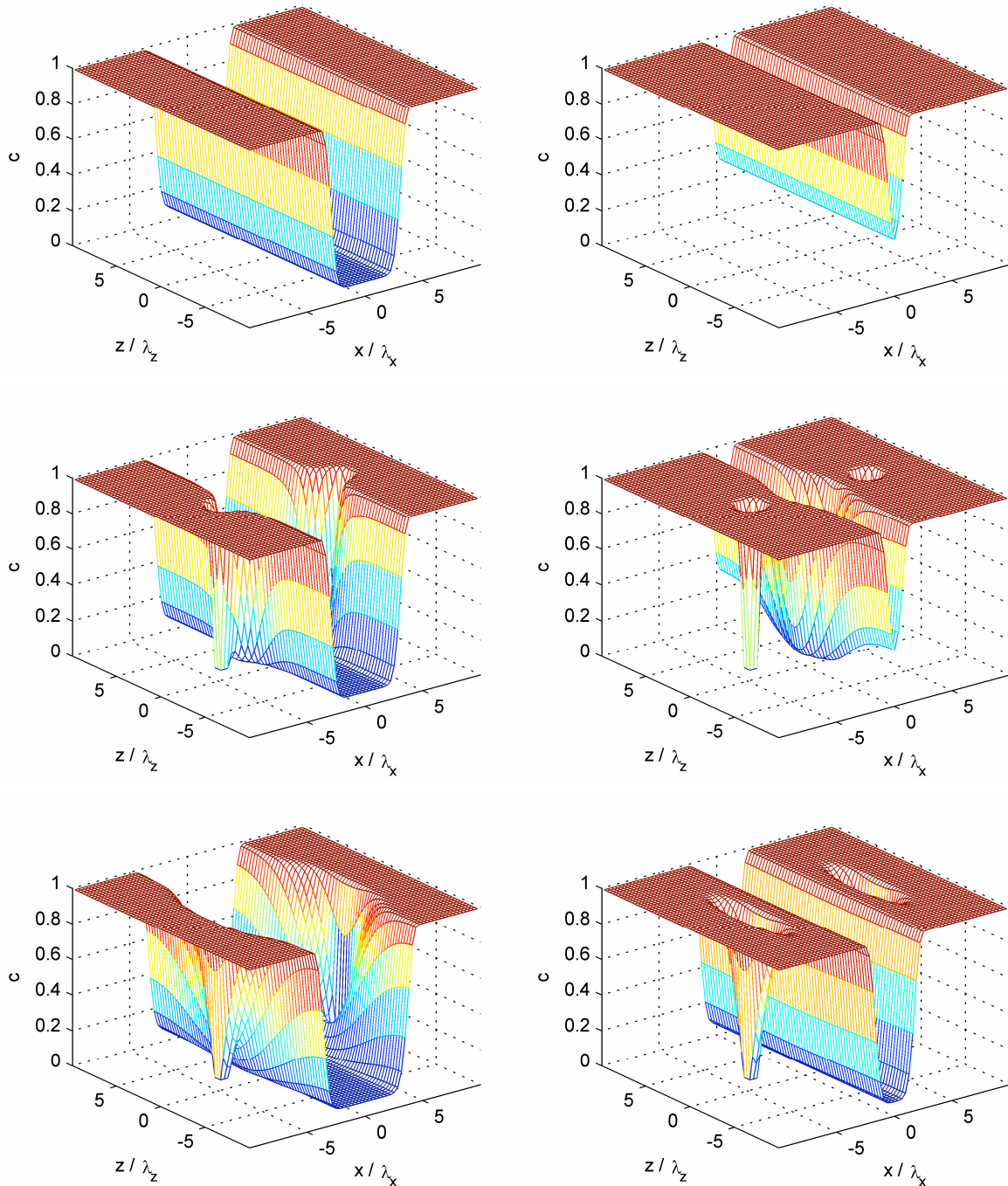


**Figure 3.** 2D simulations of lithiation dynamics. The top row shows results for a perfect (i.e. defect-free) crystal; the middle row shows results for a crystal with two defects and an isotropic gradient penalty tensor (so  $\lambda_z = \lambda_x$ ); and the third row shows results for a crystal with the same two defects as in the second case, but with an anisotropic  $K$  ( $\lambda_z = 5 \lambda_x$ ). All cases are identically nucleated by two flat, incoming waves, and are pictured at the same two time steps.

These ideas are illustrated in Fig. 3. First, note that the waves in the anisotropic crystal are much flatter than those in the isotropic one, supporting the arguments made earlier based on differential wave velocities. More significantly, by the second time step, the waves have made the most forward progress in the perfect crystal and the least forward progress in the anisotropic, defective crystal. This is reflected in Figure 2 by a sharp reduction in current while the wave interacts with the defect. To make the impact of the defect in our anisotropic case more quantitative, a 2%

reduction in the Li capacity *in this part of the crystal* has created up to a 50% drop in the Li flux *over the entire crystal*.

Note that at late times, a “hole” is left in the concentration field around the defects with approximate dimensions of  $\lambda_x \times \lambda_z$ . These can cause a crystal to suffer an even more dramatic performance degradation if there are several nearby defects. As mentioned above and discussed more rigorously in [7], the lithiation waves are stable to small-wavelength perturbations. Thus if two defects are sufficiently close, the wave can not “squeeze through” the gap between their respective holes, and they effectively become one long defect. Moreover, an array of defects with period  $\lambda_z$  can effectively block a wave, preventing the other side of the crystal from being lithiated until a new wave is nucleated.

## Conclusion

We have extended the study of phase-transformation waves in  $\text{LiFePO}_4$  initiated in [1]. In particular, we have explained how such waves propagate in more physical terms; we have shown how anisotropy in the gradient penalty tensor can predict the alignment of the phase boundary seen in experiments; and we have given preliminary results on a formal linear stability analysis. More significantly, we have shown how the model predicts a new failure mechanism for  $\text{LiFePO}_4$ : because the phase-transformation waves resist bending, they can be slowed down (or even stopped altogether) by defects in the crystal or in the nearby electrolyte. Thus even small drops in the overall Li capacity of a crystal can lead to large reductions in the power capacity. This is a result which cannot have been predicted by the shrinking core model, and once fully explored could impact the design and development of new battery systems.

## References

- [1] G. Singh, M.Z. Bazant and G. Ceder, submitted preprint. arXiv:0707.1858v1.
- [2] A.K. Padhi, K.S. Nanjundaswamy and J.B. Goodenough: J. Electrochem. Soc. Vol. 144 (1997), p. 1188
- [3] V. Srinivasan and J. Newman: J. Electrochem. Soc. Vol 151 (2004), p. A1517.
- [4] D. Morgan, A. Van der Ven and G. Ceder: ESSL Vol. 7 (2004), p. A30.
- [5] G. Chen, X. Song and T.J. Richardson: ESSL Vol. 9 (2006), p. A295.
- [6] J.W. Cahn and J.E. Hilliard: J. Chem. Phys. Vol. 28 (1958), p. 258.
- [7] D. Burch and M.Z. Bazant: in preparation.
- [8] M.S. Whittingham, Y. Song, S. Lutta, P.Y. Zavalij and N.A. Chernova: J. Mat. Chem. Vol. 15 (2005), p. 3362.